Journal of Volcanology and Geothermal Research 353 (2018) 11–17

Contents lists available at ScienceDirect

Journal of Volcanology and Geothermal Research

journal homepage: www.elsevier.com/locate/jvolgeores

# Spatial distribution of volcanic ash deposits of 2011 Puyehue-Cordón Caulle eruption in Patagonia as measured by a perturbation in NDVI temporal dynamics

Easdale M.H. [a,b,*], Bruzzone O. [a,b]

[a] Instituto Nacional de Tecnología Agropecuaria (INTA), EEA Bariloche, Av. Modesta Victoria 4450 (8400), San Carlos de Bariloche, Río Negro, Argentina
[b] Consejo Nacional de Investigaciones Científicas y Técnicas (CONICET), Argentina

ARTICLE INFO

*Article history:*
Received 4 October 2017
Received in revised form 24 January 2018
Accepted 24 January 2018
Available online 2 February 2018

*Keywords:*
Basis pursuit
Environmental hazards
Wavelet transform
MODIS
Volcanoes
Time series

ABSTRACT

Volcanic ash fallout is a recurrent environmental disturbance in forests, arid and semi-arid rangelands of Patagonia, South America. The ash deposits over large areas are responsible for several impacts on ecological processes, agricultural production and health of local communities. Public policy decision making needs monitoring information of the affected areas by ash fallout, in order to better orient social, economic and productive aids. The aim of this study was to analyze the spatial distribution of volcanic ash deposits from the eruption of Puyehue-Cordón Caulle in 2011, by identifying a sudden change in the Normalized Difference Vegetation Index (NDVI) temporal dynamics, defined as a perturbation located in the time series. We applied a sparse-wavelet transform using the Basis Pursuit algorithm to NDVI time series obtained from the Moderate Resolution Image Spectroradiometer (MODIS) sensor, to identify perturbations at a pixel level. The spatial distribution of the perturbation promoted by ash deposits in Patagonia was successfully identified and characterized by means of a perturbation in NDVI temporal dynamics. Results are encouraging for the future development of a new platform, in combination with data from forecasting models and tracking of ash cloud trajectories and dispersion, to inform stakeholders to mitigate impact of volcanic ash on agricultural production and to orient public intervention strategies after a volcanic eruption followed by ash fallout over a wide region.



## 1. Introduction

Volcanic ash fallout is a frequent environmental disturbance in forests, arid and semi-arid rangelands of Patagonia, Argentina (Inbar et al., 1995; Martin et al., 2009; Wilson et al., 2012). The ash deposits over large areas are responsible for several impacts on ecological processes such as regulation of insect populations (e.g. Fernández-Arhex et al., 2013; Masciocchi et al., 2013; Elizalde, 2014), macroinvertebrate and fish communities and dynamics of plant communities (e.g. Martin et al., 2009; Miserendino et al., 2012; Ghermandi and Gonzalez, 2012; Ghermandi et al., 2015). As well, many agricultural activities are negatively affected by the ash fallout such as in the cases of apiculture (Martínez et al., 2013) and livestock production (Easdale et al., 2014).

Livestock production is the main agricultural activity in arid and semi-arid Patagonian rangelands. The consequences of ash fallout on livestock production are i) direct (e.g. ash deposits over the body, sight problems, modifications of nutritional behavior and tooth wear, and ii) indirect impacts through the reduction of water and forage availability (Inbar et al., 1995; Wilson et al., 2010; Robles et al., 2012). These sudden changes in the environment reduces livestock productivity (i.e. worse quality of wool and less meat due to reduced offspring) and generates decapitalization due to animal death (Easdale et al., 2014), with economic and social implications. Public policy decision making needs early information of the spatial distribution of the ash fallout, highlighting the most affected zones, in order to better orient social, economic and productive aids. Then, monitoring and information about spatio-temporal durability of the perturbation and post-event recovering are crucial to support emergency response, near-real time hazard mitigation and further policy decisions.

The most frequent approaches to analyze the spatial distribution of ash deposits over large areas are: i) ground-based surveys combined with Geographical Information Systems (GIS), ii) modelling, and iii) remote sensing approaches. Ground-based surveys aimed at collecting information such as ash thickness and granulometry from several georeferenced points which are randomly distributed over a large area (e.g. Bosshard-Stadlin et al., 2014). Then, the information is analyzed

* Corresponding author at: Instituto Nacional de Tecnología Agropecuaria (INTA), EEA Bariloche, Av. Modesta Victoria 4450 (8400), San Carlos de Bariloche, Río Negro, Argentina.
*E-mail address:* easdale.marcos@inta.gob.ar (M.H. Easdale).

https://doi.org/10.1016/j.jvolgeores.2018.01.020
0377-0273/

with GIS such as interpolation methods to obtain a map with different classes that represent zones with different levels of ash deposits (e.g. Gaitán et al., 2011). This approach is costly in terms of time investment, which is difficult to implement during the early period after the eruption.

Another approach is based on modelling techniques aimed at forecasting and tracking the trajectories of ash clouds, dispersion and deposits (Webley and Mastin, 2009). For example, some proposals combine volcanic ash transport and dispersion models (VATDs), which are based on input parameters such as eruption cloud height and vertical distribution, mass eruption rate, particle size distribution and duration of the eruption (Mastin et al., 2009; Webley et al., 2009; Peterson et al., 2015). Other proposals use numerical weather predictions such as NAME model (e.g. Webster and Thomson, 2002; Witham et al., 2007; Turner et al., 2014), in which large number of model particles are released into and tracked through the computational atmosphere, using a random displacement model (Boughton et al., 1987). Other models predict ash concentration at relevant flight levels, expected deposit thickness and ash accumulation rates (Webster et al., 2012; Collini et al., 2013).

Remote sensing approaches refer to a variety of methods based on data collected by remote sensors situated on the ground, on an aircraft or a satellite such as optical sensor, radar or Lidar (Light Detection and Ranging). For example, thermal infra-red satellite data was used for ash cloud detection due to their sensitiveness to the cold temperatures of eruption clouds (Dean et al., 2004), which can be analyzed with different techniques (Tupper et al., 2004). Plume height can be estimated with satellite remote sensing data (Holasek et al., 1996) and weather radar (Oddsson et al., 2012). The Synthetic Aperture Radar (SAR) and MODIS were jointly used to assess some volcanological features of an eruption such as the relationship between surface deformation and the amount of ash and gases emitted by a volcano (Bignami et al., 2014). Volcanic ash clouds can be also tracked with airborne Lidar and in-situ measurements of aerosol and trace gases (Schumann et al., 2011). Finally, other applications of remote sensing data take advantage of the impact that ash deposits have on the reflectance of terrestrial surfaces (e.g. De Rose et al., 2011; Marzen et al., 2011; De Schutter et al., 2015). Deposits of ashes over plant communities and bare soil increases the portion of reflected radiation and reduces the photosynthetic activity of vegetation, which depends on the level of ashes covering plant photosynthetic tissues. Hence, changes in the relative proportion of reflected and absorbed radiation (i.e. red edge region) can be captured by spectral indexes such as the Normalized Differential Vegetation Index (NDVI; Tucker, 1979). Some studies compared images from different periods after the ash fallout in order to determine plant recovery rates (De Rose et al., 2011; Marzen et al., 2011). Recently, another application interpolated rainfall data in order to isolate NDVI values departing from the normal seasonal cycles, and linear temporal trends of monthly-NDVI in combination with multivariate analysis were used to identify the area over which ash fallout significantly affected vegetation (De Schutter et al., 2015). Although these are evidences supporting that ash deposits influence surface reflectance when comparing different moments or affected areas (e.g. before and after a volcanic eruption), less efforts were oriented to identify such impact by means of significant modifications in the dynamics of spectral indexes from a time series approach.

The aim of this study is to analyze the spatial distribution of volcanic ash deposits of 2011 eruption of Puyehue-Cordón Caulle Volcanic Complex in Patagonia as measured by the identification of sudden changes in NDVI temporal dynamics. In particular, we used time series analysis based on a sparse-wavelet transform to identify perturbations in NDVI time series at a pixel level using MODIS data. This approach can provide a new platform to inform stakeholders to mitigate impact of volcanic ash on agricultural production on a country-scale, and decision makers to orient intervention strategies after a volcanic eruption followed by ash fallout over a wide region.

## 2. Materials and methods

### 2.1. Study area and volcanic eruption event

The region of study was North Patagonia, including Argentina and Chile. The geomorphology of this region is dominated by the Andean range towards the West (across the international limit), hills and basaltic plateaus in inner Argentinean Patagonia, and great arid plains towards the East. Climate is Mediterranean with mean annual precipitation that ranges between over 4000 mm (W) to 150 mm (E), falling in autumn and winter. Mean annual temperature ranges spatially from 8° (W) to 12° (E) (Paruelo et al., 1998; Bran et al., 2000). Vegetation is dominated by forest of *Nothofagus* spp. in the Andean mountains. Semiarid rangelands of western and central zones of the study area (i.e. Subandean steppes, Patagonian Western District and Patagonian Central District, León et al., 1998; Bran et al., 2000) are dominated by low shrub-grass steppes of *Mulinum spinosum*, *Senecio* spp. and *Pappostipa speciosa*, and low shrub steppes dominated by *Nassauvia* spp. and *Chuquiraga avellanedae*. The eastern rangelands (i.e. Monte Austral, León et al., 1998) are dominated by medium shrub-grass steppes of *Larrea* spp., *Prosopis denudans*, *Atriplex lampa*, *Lycium* spp. and *Pappostipa humilis* (Cabrera, 1971; León et al., 1998). The agrarian structure is a matrix dominated by smallholders, with capitalized family-based farms and commercial farms. The dominant husbandry across different farm types in arid and semiarid rangelands is sheep mixed with goats in less capitalized farms, and with cattle in more capitalized and commercial farms (Easdale et al., 2009).

We studied the impact of the well documented eruption of the Puyehue-Cordón Caulle Volcanic Complex (PCCVC; 40°35′ S, 72°07′ W), which occurred on 4th June 2011. During the initial phase of the eruption (first 24 h), a 14-km-high plume dispersed a large volume of rhyolitic tephra over a wide area eastward towards Argentina. The resulting tephra deposits consisted of 13 main layers grouped into four units, whereas most of the tephra was emitted during the first 72 h of the event. The lowest part of the eruptive sequence, which recorded the highest intensity phase, was composed of alternating lapilli layers with a total estimated volume of ca. 0.75 $km^3$ (Pistolesi et al., 2015). We selected this eruption event because of the wide area affected by ash fallout in the North-western portion of Patagonia, Argentina (Gaitán et al., 2011). Since we were interested in the impact of ash depositions and the consequently modifications of surface reflectance, we selected this event because the main impact occurred across different ecological and geomorphological zones.

### 2.2. Data source

The Normalized Difference Vegetation Index (NDVI) is frequently used as a surrogate of ecosystem primary production, since it is an accurate indicator of the level of photosynthetic activity of vegetation (Tucker, 1979; Ruimy et al., 1994). We used the 2000 to mid-2017-time series of 16-day temporal resolution and 250 m spatial resolution of NDVI to study the perturbations in NDVI dynamics generated by the ash deposits after the volcanic eruption.

The NDVI was derived from Moderate Resolution Image Spectroradiometer (MODIS) sensor (product MOD13Q1). NDVI was calculated with the following equation:

$$NDVI = (NIR - R)/(NIR + R) \quad (1)$$

where R and NIR are the surface reflectances centered at 645 nm (visible) and 858 nm (near-infrared) portions of the electromagnetic spectrum, respectively.

### 2.3. Data processing

Because NDVI is a continuous finite variable, we assumed that the NDVI error followed a logit-normal distribution (i.e. a statistical distribution whose logit transform follows a normal distribution). Therefore, before fitting the NDVI time series, temporal data were logit-transformed in order to use a normal likelihood function. Since NDVI is a value between −1 and 1, but values lower than 0 do not have a biological meaning (i.e. values below zero mean snow cover, clouds, water or rocks), we treated it in a similar way as a proportion between 0 and 1. Logit transformation also avoids the use of the more complex Beta distribution as a likelihood function. Instead we used a normal function, which is also simpler in interpretation in terms of mean and variance. A second benefit was to avoid dealing with meaningless values (i.e. estimated values larger than 1 or lower than zero).

After the transformation of NDVI data, we centered the series by removing the mean. Values lower than zero, as well as data with quality indicator different than zero or one, were treated as missing values. If a pixel in the data stack consisting of *xy* NDVI layers contained a proportion of >1/4 negative values, it was discarded from the analysis. After this procedure, most of the discarded pixels corresponded to borders of water bodies and top of the mountains. Once the model-fitting procedure was finished we transformed the fitted values back to the original NDVI scale by using an inverse logit transform, so the results are all expressed in NDVI units.

### 2.4. Time series analysis

To assess the impact of the ash fall, we decomposed the NDVI time series variability by using a wavelet analysis. We performed a sparse-wavelet transform using the *Basis Pursuit* algorithm (Chen et al., 2001), because it provides a more parsimonious representation of the variability contained in the time series. In particular, this procedure maximizes variability representation with the minimum number of parameters.

*Basis Pursuit* is a sparse dictionary learning method, in which the data is represented as a linear combination of basic elements called *atoms*, here named a Gabor function (Gabor, 1946). These functions are cosine functions multiplied by a Gaussian window. As a result, the signal is depicted by a sum of functions whose properties are localized in a time dimension (center of the Gaussian window), width (the standard deviation of the underlying Gaussian function, in years), frequency of the cosine function (1 year$^{-1}$), and amplitude in NDVI units.

The atoms were fitted to the time series with a stepwise procedure by using the L-BFGS algorithm (Liu and Nocedal, 1989). After fitting each atom, it was removed from the time series and a new atom was then fitted to residuals, according to the InCrowd algorithm (Gill et al., 2011). The procedure was repeated as long as the Akaike Information Criterion (AIC) decreased. Once the AIC index increased, we stopped the procedure and the fitted atoms were kept for the following steps. To avoid issues related to the lack of independence of data found in time series, an autoregressive model with conditional heteroscedasticity (ARCH model; Brockwell and Davis, 2016) was used for modelling the errors during the fitting of atoms.

We aimed at analyzing a sudden and significant modification in NDVI temporal dynamics, which represented a tephra deposition. Hence, after performing the *Basis Pursuit* procedure, we filtered the atoms in search for the ones whose frequency corresponded to: i) a wavelength longer than the window width (i.e. a kind of "bump" in the time series), ii) window width shorter than 1/4 of the time series length, and iii) negative amplitude, meaning the pattern of a negative perturbation with limited duration in the time series (i.e. a negative perturbation with a subsequent recuperation within the time span of the study). We estimated the following parameters: amplitude as a measure of intensity (integral of impact), temporal extent (length of impact) and localization in time of the perturbation (mean point of impact), which were the parameters of the Gabor functions obtained after filtering (Fig. 1).

Perturbation power was measured in *decibels* (*dB*) (Van Valkenburg, 2001), with $dB = 10\,log_{10}(P_p/P_{wn})$, being $P_p$, the covariance between the data, and the perturbation function (the grey area in Fig. 1), $P_{wn}$ the

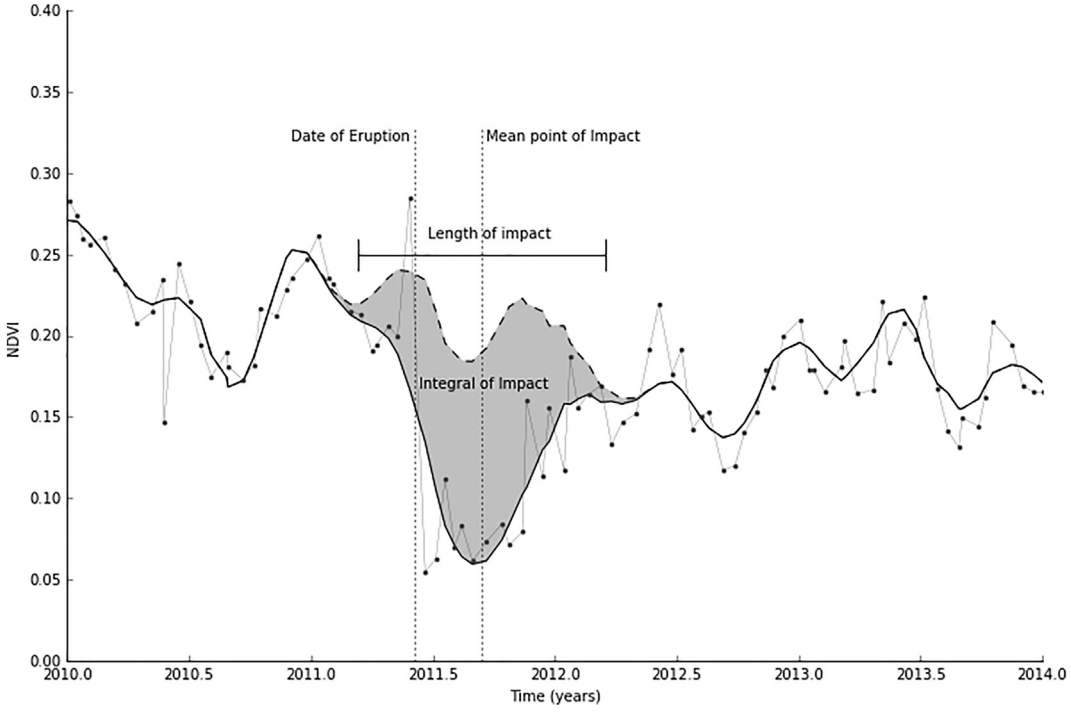


**Fig. 1.** Example of a pixel with the pattern of NDVI perturbation. Parameters of the Gabor function: i) Amplitude (Integral of impact), ii) Temporal extent (Length of impact), and iii) Localization of the perturbation in time (Mean point of impact) and Date of eruption (4th June 2011). Black dots and grey lines identify original data, black full line identify the estimate of the function including the perturbation and cut line an hypothetical function without the perturbation.

variance of the white noise, which are the data residuals after filtering out all the Gabor atoms and the autoregressive model.

In order to identify the spatial distribution of pixels which contained the explained pattern of perturbation, we assigned a grey color-scale according to the gradient of perturbation power, where increasingly dark grey referred to higher negative values. This map was overlapped with two different sources of information available for North Patagonia to associate the NDVI perturbation patterns with ash deposits and biophysical heterogeneity (e.g. forest, steppes): a) areas with similar thickness of ash deposits estimated with ground-based data (Gaitán et al., 2011); b) regional ecological areas of North Patagonia, Argentina (Bran et al., 2000, 2002).

Given the enormous amount of data to be processed, we performed the basis pursuit procedure, using an OpenCL version 1.1 (Kronos Group, 2011) via pyopencl (Klöckner et al., 2012), on Nvidia geforce 680, AMD Radeon 7870 and AMD Radeon R9 290x GPUs. The filtering and the remainder data processing was performed using the python programming language (Van Rossum and Drake, 2003), with the numpy libraries for numerical computation (Oliphant, 2006). Data processing speed was 474 $km^2$ per minute, which means that overall time required to process the study area was one day.

## 3. Results

A perturbation event was recorded for the year 2011 over a large area in Patagonia, with a NW-SE spatial distribution (Fig. 2).

The total area that significantly recorded a NDVI perturbation pattern in the year 2011 (Fig. 3) followed a normal distribution (Fig. 4), and the spatial distribution was estimated in 21,059 $km^2$ across three provinces of Patagonia, Argentina (Fig. 2).

The intensity of NDVI perturbation pattern, as measured by perturbation power, was associated to ash thickness, in arid and semi-arid rangelands from inner Patagonia and across different ecological regions. However, the areas with thicker ash deposits (>5 cm; Gaitán et al., 2011) associated to Andean forests did not recorded changes, except for the forest zones near the volcanic chain, were eruption occurred (Fig. 5).

## 4. Discussion

The spatial distribution of the perturbation promoted by ash deposits in Patagonia from the volcanic eruption of Puyehue-Cordón Caulle Volcanic Complex in 2011 was successfully identified by means of a sudden change in NDVI temporal dynamics. The NDVI perturbation pattern was identified in a NW-SE spatial distribution from the location of the eruption, which concur with the main ash dispersion in the highest intensity phase, during which a bent-over plume dispersed tephra towards the southeast-east, as far as the Atlantic Ocean (Pistolesi et al., 2015). The most affected areas were arid and semi-arid rangelands from inner Patagonia, whereas the Andean forests did not showed changes. This pattern suggests that ash deposits effectively increased the portion of surface reflectance and reduced the photosynthetic activity of vegetation in areas with medium to short vegetation heights (i.e. shrub-grass steppes), and high proportions of bare soil (varying spatially from 40 to 60%) (De Rose et al., 2011; Marzen et al., 2011). On the other hand, the used remote sensing data were much less sensitive to changes promoted by ash deposits in the forest areas (del Moral and Grishin, 1999; Ayris and Delmelle, 2012). This might be due to the canopy structure. Forests can mask the reflectance of ash particles due to their thick crown regions of evergreen tree species, whereas ash deposits remained mostly below the foliage in the following spring and summer. In addition, the eruption occurred in the winter and some tree species of the study area are deciduous, which means a marginal impact of ash deposits on these tree canopies. The only exception occurred in a zone near the volcanic chain, where forest was significantly influenced by thicker and hotter ash depositions, which affected the survival and productivity of trees in the following growing season (Fig. 5, Chile). These patterns are in line with a long-lived discussion in remote sensing on the Leaf Area Index (LAI), soil reflectance and its impact on vegetation indices. Results corroborate that soil spectral properties were much more variable in the context of ash depositions

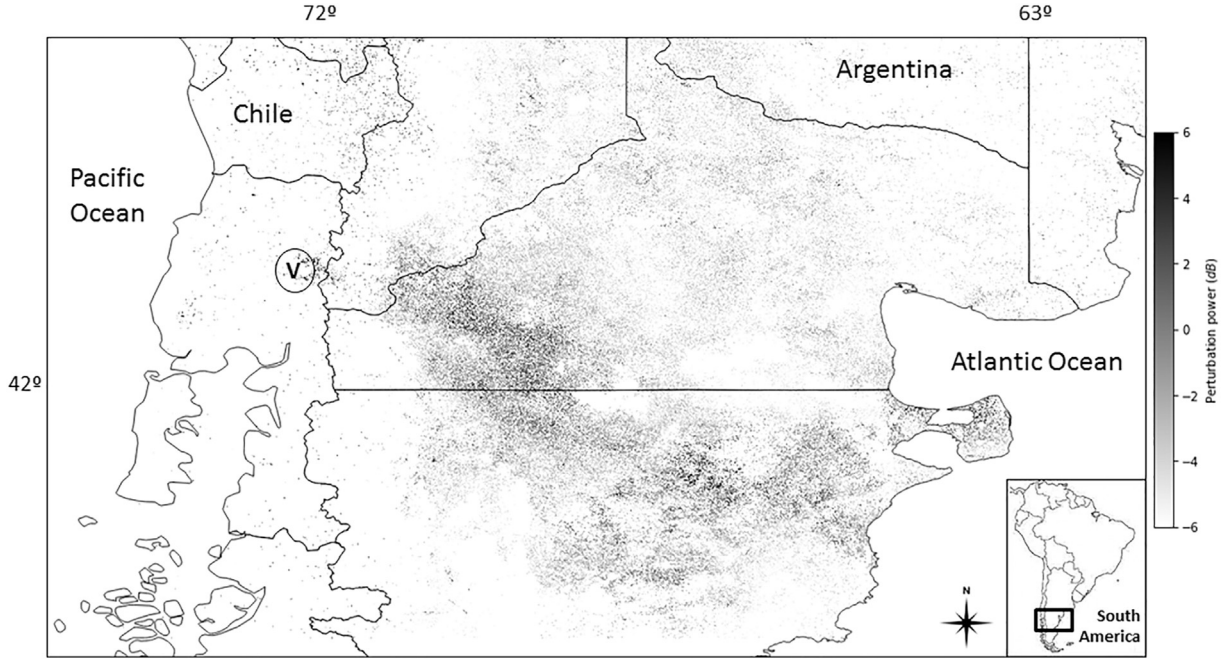


**Fig. 2.** Spatial distribution of a perturbation in NDVI time series in the year 2011 in Patagonia, South America. Each dot represents a pixel (6.25 ha) and a grey scale was used to identify the gradient of perturbation power (see Fig. 3), where increasingly dark grey refers to higher values and white means no perturbation pattern. Letter V within a circle identifies the location of Puyehue-Cordón Caulle Volcanic Complex, Chile. A black rectangle in South America identifies the study area.

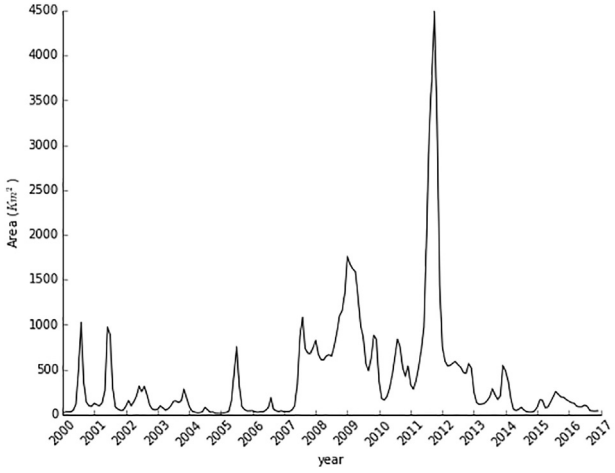


**Fig. 3.** Total area by year of perturbation in NDVI time series as measured by the position of the minimum value (i.e. mean point of impact, Fig. 1). Each datum refers to a pixel of 6.25 ha.

in sparse vegetation cover areas (e.g. grassland and shrublands) than in zones with higher LAI such as evergreen forests (Montandon and Small, 2008). Whereas there are also other indices available that can adjust for soil exposure and LAI (e.g. Soil-Adjusted Vegetation Index –SAVI-; Huete, 1988), more significant advances are still required in data about the spatial distribution and temporal variation of soil reflectance. The identified spatial variation of NDVI temporal perturbations can serve as a source of information to orient future research on surface reflectance features. In particular, studies of modifications due to tephra depositions after an eruption and their forwarding spatial remobilization dynamic by wind (Panebianco et al., 2017) in Patagonia.

Remote sensing data are primary sources extensively used for change detection of Earth's surface features in recent decades and many techniques are in the core of developments and debate for this end (Lu et al., 2004; Mishra et al., 2016). We applied a sparse-wavelet transform using the Basis Pursuit algorithm, which was sensitive to capture NDVI perturbation patterns with a very high data processing speed. This method provided an accurate temporal representation of the perturbation, with a high spatial resolution and a complete picture of the spatial distribution of ash deposits which affected vegetation dynamics, as a measure of the impact on large regions such as arid and semi-arid rangelands of Patagonia. In particular, the method provided additional spatial information to already known impact of ash deposits on Patagonia (e.g. Easdale et al., 2014; Bignami et al., 2014). The total area and boundaries of affected zones were defined at a high spatial resolution (250 m) and without interpolation. Previous studies based on ground-based data estimated that ash fallout covered an area of over 3 million ha in the North-western portion of Patagonia, Argentina (Gaitán et al., 2011). Whereas the boundaries of the affected zones mostly coincided with this study (Fig. 5a), the main difference was located in the resolution of information, since an intensity gradient of the perturbation that affected vegetation dynamics was better identified. Although the relationship between NDVI perturbation power and threshold detection of ash thickness was not tackled by this study and should need further research, the results suggest that detection of changes in surface reflectance at a pixel level may be highly accurate, since a 1.5 cm-boundary between Zones B and C was successfully depicted (Fig. 5a). This suggest a promising resolution in comparison with other available methods (De Schutter et al., 2015).

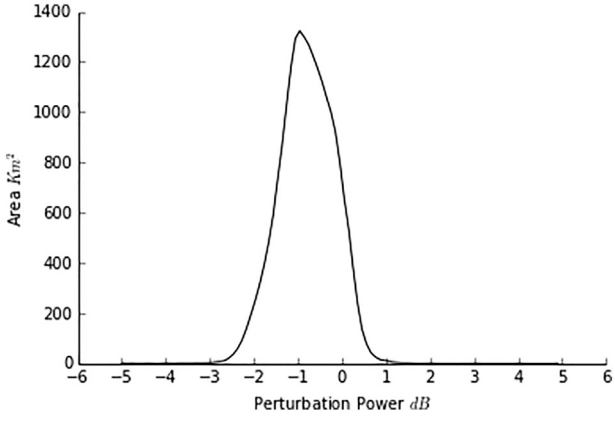


**Fig. 4.** Total area classified by perturbation power for the year 2011 (measured in decibels, dB) in NDVI time series. Each datum refers to a pixel of 6.25 ha.

The grain of information suggests that a more accurate impact assessment of ash deposits over economic activities such as livestock production can be made (i.e. farm level, landscape units), taking advantage of the high temporal and spatial resolution of some satellite imageries. Hence, these results are encouraging as a potential method to delimitate zones affected by volcanic eruptions followed by ash fallout in Patagonia and analogous regions. However, some challenges were identified as bottlenecks to early inform spatial distribution of ash deposit near-after a volcanic eruption. Firstly, perturbations were depicted by the integration of the negative impact as well as recovery in NDVI temporal behavior, which means that information would not be immediately available after an eruption event. In this respect, the main advantages can be obtained by combining the results of these procedures with outcomes from forecasting models of ash cloud trajectory, dispersion and deposition. Secondly, the usage of optic sensor-based data and the Basis Pursuit algorithm were most sensitive in arid and semi-arid rangelands, suggesting higher opportunities in such environments for the development of a monitoring system. However, this method was less sensitive in forest and mountainous areas. Further research is needed to take advantage of the combination of thermal infrared data (TIR) from optic sensors and microwave data obtained from radar sensors to enhance ash detection in cloudy sky conditions (Bignami et al., 2014) and over areas with high LAI such as forests. The kind of information obtained by the proposed procedure, should complement ground-based data and modelling techniques as a corroboration of predicted information such as expected ash deposition areas. The outcomes of these applications can contribute to better orient policy intervention such as State aids for livestock production and rural population, as well as post-event farming decision making.

Environmental perturbations can be addressed through the lens of time series analysis of spectral indexes such as NDVI (Illera et al., 1996). In this regard, the proposed method can be used to analyze the spatial distribution of other kind of disturbances affecting surface reflectance such as fires or droughts, which may complement other perspectives such as behavioral dynamic trends (Telesca and Lasaponara, 2006; Easdale et al., 2018). Further research is needed to integrate ground-based surveys combined with geographic analysis and dynamic perspectives based on remote sensing data, in order to fully capture the impact of disturbances such as ash fallout in large areas.

## 5. Conclusion

The spatial distribution of the perturbation promoted by ash deposits in Patagonia from the volcanic eruption of Puyehue-Cordón Caulle Volcanic Complex in 2011 was successfully identified by means of a sudden change in NDVI temporal dynamics. The sparse-wavelet transform using the Basis Pursuit algorithm was sensitive to capture this perturbation. This process was done by keeping a high data resolution (250 m) and was performed for a large area with a high processing speed. Future steps should combine this kind of information with outcomes from forecasting and tracking models of ash cloud trajectory, dispersion and deposition. These results are encouraging for the future development of a new platform to inform stakeholders to mitigate

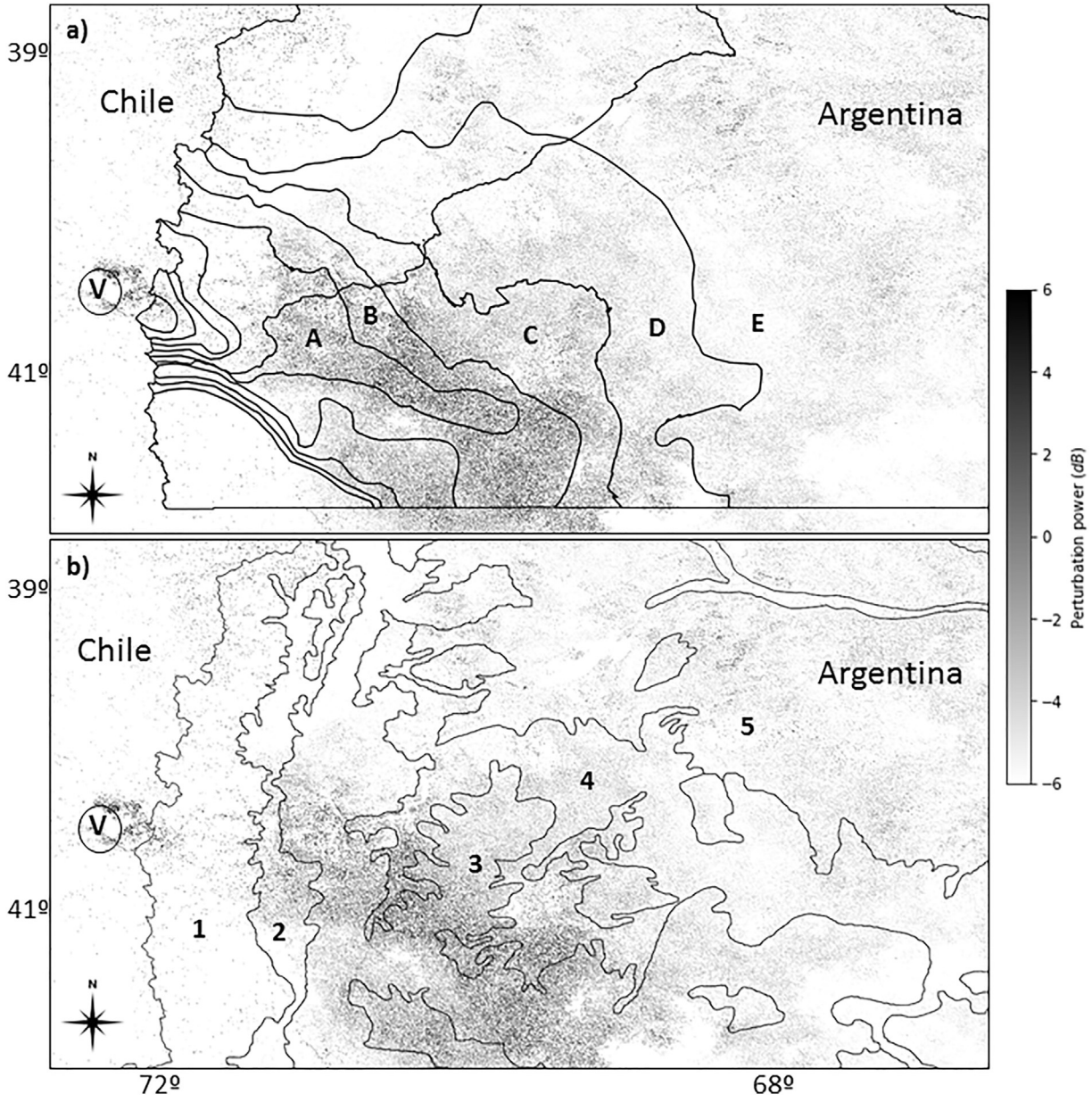


**Fig. 5.** Spatial distribution of perturbation in NDVI time series and a) areas with similar thickness of ash deposits estimated with ground-based data (Gaitán et al., 2011), ash thickness classes: A: 5.0 to 3.0 cm; B: 3.0 to 1.5 cm; C: 1.5 to 0.5 cm; D: 0.5 to 0.1; E: Not affected; b) regional ecological areas in Patagonia, Argentina (Bran et al., 2000, 2002), 1) Andean Mountains with forest, 2) Subandean steppes, 3) Patagonian Western District, 4) Patagonian Central District, 5) Monte Austral. Letter V within a circle identifies the location of Puyehue-Cordón Caulle Volcanic Complex, Chile.

impact of volcanic ash on agricultural production and for decision makers to orient intervention strategies after a volcanic eruption followed by ash fallout over a wide region.

## Acknowledgments

This research was supported by Instituto Nacional de Tecnología Agropecuaria (INTA) under grants PRET-1281102 and PRET-1281103. We thank two anonymous reviewers for their suggestions, which enriched the content and improved the readability of this paper.

## References

Ayris, P.M., Delmelle, P., 2012. The immediate environmental effects of tephra emission. Bull. Volcanol. 74, 1905–1936.

Bignami, C., Corradini, S., Merucci, L., De Michele, M., Raucoules, D., De Astis, G., Stramondo, S., Piedra, J., 2014. Multisensor satellite monitoring of the 2011 Puyehue-Cordon Caulle eruption. IEEE J. Sel. Top. Appl. Earth Obs. Remote Sens. 7 (7), 2786–2796.

Bosshard-Stadlin, S.A., Mattsson, H.B., Keller, J., 2014. Magma mixing and forced exsolution of $CO_2$ during the explosive 2007–2008 eruption of Oldoinyo Lengai (Tanzania). J. Volcanol. Geotherm. Res. 285, 229–246.

Boughton, B.A., Delaurentis, J.M., Dunn, W.E., 1987. A stochastic-model of particle dispersion in the atmosphere. Bound.-Layer Meteorol. 40, 147–163.

Bran, D., Ayesa, J., Lopez, C., 2000. Regiones Ecológicas de Río Negro. Comunicación Técnica 59. INTA, EEA, Bariloche, Río Negro, Argentina.

Bran, D., Ayesa, J., López, C., 2002. Áreas Ecológicas de Neuquén. Comunicación Técnica, Área de Recursos Naturales. INTA, EEA Bariloche (8pp.).

Brockwell, P.J., Davis, R.A., 2016. Introduction to Time Series and Forecasting. Springer.

Cabrera, A., 1971. Fitogeografía de la República Argentina. Bol. Soc. Argent. Bot. 14, 1–42.

Chen, S.S., Donoho, D.L., Saunders, M.A., 2001. Atomic decomposition by basis pursuit. SIAM Rev. 43, 129–159.

Collini, E., Osores, M.S., Folch, A., Viramonte, J.G., Villarosa, G., Salmuni, G., 2013. Volcanic ash forecast during the June 2011 Cordón Caulle eruption. Nat. Hazards 66 (2), 389–412.

De Rose, R.C., Oguchi, T., Morishima, W., Collado, M., 2011. Land cover change on Mt. Pinatubo, the Philippines, monitored using ASTER VNIR. Int. J. Remote Sens. 32 (24), 9279–9305.

De Schutter, A., Kervyn, M., Canters, F., Bosshard-Stadlin, S.A., Songo, M.A.M., Mattsson, H. B., 2015. Ash fall impact on vegetation: a remote sensing approach of the Oldoinyo Lengai 2007–08 eruption. J. Appl. Volcanol. 4 (1), 15.
Dean, K.G., Dehn, J., Papp, K.P., Smith, S., Izbekov, P., Peterson, R., Kearney, C., Steffke, A., 2004. Integrated satellite observations of the 2001 eruption of Mt. Cleveland, Alaska. J. Volcanol. Geotherm. Res. 135, 51–73.
Easdale, M.H., Aguiar, M.R., Román, M., Villagra, S.E., 2009. Comparación socio-económica de dos regiones biofísicas: los sistemas ganaderos de la provincia de Río Negro, Argentina. Cuad. Desarro. Rural 62, 173–198.
Easdale, M.H., Sacchero, D., Vigna, M., Willems, P., 2014. Assessing the magnitude of impact of volcanic ash deposits on Merino wool production and fibre traits in the context of a drought in North-west Patagonia, Argentina. Rangel. J. 36 (2), 143–149.
Easdale, M.H., Bruzzone, O., Mapfumo, P., Tittonell, P., 2018. Phases or regimes? Revisiting NDVI trends as proxies for land degradation. Land Degrad. Dev. https://doi.org/10.1002/ldr.2871 (In press).
Elizalde, L., 2014. Volcanism and arthropods: a review. Ecol. Austral 24 (1), 3–16.
Fernández-Arhex, V., Buteler, M., Amadio, M.E., Enriquez, A., Pietrantuono, A.L., Stadler, T., Becker, G., Bruzzone, O., 2013. The effects of volcanic ash from Puyehue-Caulle range eruption on the survival of Dichroplus vittigerum (Orthoptera: Acrididae). Fla. Entomol. 96 (1), 286–288.
Gabor, D., 1946. Theory of communication. Part 1: the analysis of information. J. Inst. Electr. Eng. III: Radio Commun. Eng. 93, 429.
Gaitán, J.J., Ayesa, J.A., Umaña, F., Raffo, F., Bran, D.B., 2011. Cartography of the Area Affected by Volcanic Ash Deposits inthe Provinces of Neuquén and Río Negro. INTA Bariloche, RíoNegro, Argentina.
Ghermandi, L., Gonzalez, S., 2012. Early observations of volcanic ash deposition and its impact on the vegetation steppes of NW Patagonia. Ecol. Austral 22 (2), 144–149.
Ghermandi, L., Gonzalez, S., Franzese, J., Oddi, F., 2015. Effects of volcanic ash deposition on the early recovery of gap vegetation in Northwestern Patagonian steppes. J. Arid Environ. 122, 154–160.
Gill, P.R., Wang, A., Molnar, A., 2011. The in-crowd algorithm for fast basis pursuit denoising. IEEE Trans. Signal Process. 59, 4595–4605.
Holasek, R.E., Self, S., Woods, A.W., 1996. Satellite observations and interpretation of the 1991 Mount Pinatubo plumes. J. Geophys. Res. 101 (B12), 27,365–27,655.
Huete, A.R., 1988. A soil-adjusted vegetation index (SAVI). Remote Sens. Environ. 25 (3), 295–309.
Illera, P., Fernandez, A., Delgado, J.A., 1996. Temporal evolution of the NDVI as an indicator of forest fire danger. Int. J. Remote Sens. 17 (6), 1093–1105.
Inbar, M., Ostera, H.A., Parica, C.A., Remesal, M.B., Salani, F.M., 1995. Environmental assessment of 1991 Hudson volcano eruption ashfall effects on southern Patagonia region, Argentina. Environ. Geol. 25 (2), 119–125.
Khronos OpenCL Working Group, 2011. The OpenCL specification version 1.1. http://www.khronos.org/registry/cl/specs/opencl-1.1.
Klöckner, A., Pinto, N., Lee, Y., Catanzaro, B., Ivanov, P., Fasih, A., 2012. PyCUDA and PyOpenCL: a scripting-based approach to GPU run-time code generation. Parallel Comput. 38, 157–174.
León, R., Bran, D., Collantes, M., Paruelo, J.M., Soriano, A., 1998. Grandes Unidades de Vegetación de la Patagonia. Ecol. Aust. 8 (2), 125–144.
Liu, D.C., Nocedal, J., 1989. On the limited memory BFGS method for large scale optimization. Math. Program. 45 (1), 503–528.
Lu, D., Mausel, P., Brondizio, E., Moran, E., 2004. Change detection techniques. Int. J. Remote Sens. 25 (12), 2365–2401.
Martin, R.S., Watt, S.F.L., Pyle, D.M., Mather, T.A., Matthews, N.E., Georg, R.B., Day, J.A., Fairhead, T., Witt, M.L.I., Quayle, B.M., 2009. Environmental effects of ashfall in Argentina from the 2008 Chaitén volcanic eruption. J. Volcanol. Geotherm. Res. 184 (3), 462–472.
Martínez, A.S., Masciocchi, M., Villacide, J.M., Huerta, G., Daneri, L., Bruchhausen, A., Rozas, G., Corley, J.C., 2013. Ashes in the air: the effects of volcanic ash emissions on plant-pollinator relationships and possible consequences for apiculture. Apidologie 44, 268–277.
Marzen, L.J., Szantoi, Z., Harrington, L.M., Harrington Jr, J.A., 2011. Implications of management strategies and vegetation change in the Mount St. Helens blast zone. Geocarto Int. 26 (5), 359–376.
Masciocchi, M., Pereira, A.J., Lantschner, M.V., Corley, J.C., 2013. Of volcanoes and insects: the impact of the Puyehue–Cordon Caulle ash fall on populations of invasive social wasps, *Vespula* spp. Ecol. Res. 28 (2), 199–205.
Mastin, L.G., Guffanti, M., Servranckx, R., Webley, P., Barsotti, S., Dean, K., Durant, A., Ewert, J.W., Neri, A., Rose, W.I., Schneider, D.A., 2009. A multidisciplinary effort to assign realistic source parameters to models of volcanic ash-cloud transport and dispersion during eruptions. J. Volcanol. Geotherm. Res. 186 (1), 10–21.
Miserendino, M.L., Archangelsky, M., Brand, C., Epele, L.B., 2012. Environmental changes and macroinvertebrate responses in Patagonian streams (Argentina) to ashfall from the Chaitén Volcano (May 2008). Sci. Total Environ. 424, 202–212.
Mishra, S., Shrivastava, P., Dhurvey, P., 2016. Change detection techniques in remote sensing. J. Adv. Inf. Technol. Converg. 6 (2), 51–57.
Montandon, L.M., Small, E.E., 2008. The impact of soil reflectance on the quantification of the green vegetation fraction from NDVI. Remote Sens. Environ. 112 (4), 1835–1845.
del Moral, R., Grishin, S.Y., 1999. Volcanic disturbances and ecosystem recovery. In: Walker, L.R. (Ed.), Ecosystems of Disturbed Ground. Elsevier Science, pp. 137–154.
Oddsson, B., Gudmundsson, M.T., Larsen, G., Karlsdóttir, S., 2012. Monitoring of the plume from the basaltic phreatomagnetic 2004 Grímsvötn eruption-application of weather radar and comparison with plume models. Bull. Volcanol. 74, 1395–1407.
Oliphant, T.E., 2006. A Guide to NumPy. Trelgol Publishing, USA, p. 85.
Panebianco, J.E., Mendez, M.J., Buschiazzo, D.E., Bran, D., Gaitán, J.J., 2017. Dynamics of volcanic ash remobilisation by wind through the Patagonian steppe after the eruption of Cordón Caulle, 2011. Sci. Rep. 7.
Paruelo, J.M., Jobbágy, E., Sala, O., 1998. Biozones of Patagonia (Argentina). Ecol. Aust. 8, 145–153.
Peterson, R., Webley, P., D'Amours, R., Servranckx, R., Stunder, B., Papp, K., 2015. Volcanic ash transport and dispersion models. In: Dean, K.G., Dehn, J. (Eds.), Monitoring Volcanoes in the North Pacific. Springer Praxis Books, Springer, Berlin, Heidelberg.
Pistolesi, M., Cioni, R., Bonadonna, C., Elissondo, M., Baumann, V., Bertagnini, A., Chiari, L., Gonzales, R., Rosi, M., Francalanci, L., 2015. Complex dynamics of small-moderate volcanic events: the example of the 2011 rhyolitic Cordón Caulle eruption, Chile. Bull. Volcanol. 77 (1), 3.
Robles, C.A., Cabrera, R., Martínez, A., 2012. Tooth wear in sheep after the Puyehue-Caulle Cordon eruption. II Patagonian Veterinary Congress: Bariloche, Argentina.
Ruimy, A., Saugier, B., Dedieu, G., 1994. Methodology for the estimation of terrestrial net primary production from remotely sensed data. J. Geophys. Res. 99, 5263–5283.
Schumann, U., Weinzierl, B., Reitebuch, O., Schlager, H., Minikin, A., Forster, C., Baumann, R., Sailer, T., Graf, K., Mannstein, H., Voigt, C., Rahm, S., Simmet, R., Scheibe, M., Lichtenstern, M., Stock, P., Rüba, H., Schäuble, D., Tafferner, A., Rautenhaus, M., Gerz, T., Ziereis, H., Krautstrunk, M., Mallaun, C., Gayet, J.-F., Lieke, K., Kandler, K., Ebert, M., Weinbruch, S., Stohl, A., Gasteiger, J., Groß, S., Freudenthaler, V., Wiegner, M., Ansmann, A., Tesche, M., Olafsson, H., Sturm, K., 2011. Airborne observations of the Eyjafjalla volcano ash cloud over Europe during air space closure in April and May 2010. Atmos. Chem. Phys. Discuss. 11, 2245–2279.
Telesca, L., Lasaponara, R., 2006. Pre-and post-fire behavioral trends revealed in satellite NDVI time series. Geophys. Res. Lett. 33 (14).
Tucker, C.J., 1979. Red and photographic infrared linear combinations for monitoring vegetation. Remote Sens. Environ. 8, 127–150.
Tupper, A., Carn, S., Davey, J., Kamada, Y., Potts, R., Prata, F., Tokuno, M., 2004. An evaluation of volcanic cloud detection techniques during recent significant eruptions in the western 'ring of fire'. Remote Sens. Environ. 91, 27–46.
Turner, R., Moore, S., Pardo, N., Kereszturi, G., Uddstrom, M., Hurst, T., Cronin, S., 2014. The use of Numerical Weather Prediction and a Lagrangian transport (NAME-III) and dispersion (ASHFALL) models to explain patterns of observed ash deposition and dispersion following the August 2012 Te Maari, New Zealand eruption. J. Volcanol. Geotherm. Res. 286, 437–451.
Van Rossum, G., Drake, F.L., 2003. Python language reference manual. Network Theory, p. 144.
Van Valkenburg, M.E., 2001. Reference Data for Engineers: Radio, Electronics, Computers and Communications. Newnes.
Webley, P., Mastin, L., 2009. Improved prediction and tracking of volcanic ash clouds. J. Volcanol. Geotherm. Res. 186, 1–9.
Webley, P.W., Stunder, B.J., Dean, K.G., 2009. Preliminary sensitivity study of eruption source parameters for operational volcanic ash cloud transport and dispersion models—a case study of the August 1992 eruption of the Crater Peak vent, Mount Spurr, Alaska. J. Volcanol. Geotherm. Res. 186 (1), 108–119.
Webster, H.N., Thomson, D.J., 2002. Validation of a Lagrangian model plume rise scheme using the Kincaid data set. Atmos. Environ. 36, 5031–5042.
Webster, H.N., Thomson, D.J., Johnson, B.T., Heard, I.P., Turnbull, K., Marenco, F., Kristiansen, N.I., Dorsey, J., Minikin, A., Weinzierl, B., Schumann, U., 2012. Operational prediction of ash concentrations in the distal volcanic cloud from the 2010 Eyjafjallajökull eruption. J. Geophys. Res. Atmos. 27 (117(D20)).
Wilson, T., Steward, C., Cole, J., Johnston, D., Cronin, S., 2010. Vulnerability of farm water supply systems to volcanic ash fall. Environ. Earth Sci. 61:675–688. https://doi.org/10.1007/s12665-009-0380-2.
Wilson, T., Cole, J., Johnston, D., Cronin, S., Stewart, C., Dantas, A., 2012. Short-and long-term evacuation of people and livestock during a volcanic crisis: lessons from the 1991 eruption of Volcán Hudson, Chile. J. Appl. Volcanol. 1 (2), 1–11.
Witham, C.S., Hort, M.C., Potts, R., Servranckx, R., Husson, P., Bonnardot, F., 2007. Comparison of VAAC atmospheric dispersion models using the 1 November 2004 Grimsvötn eruption. Meteorol. Appl. 14, 27–38.